TMK-based cell surface auxin signaling activates cell wall acidification in Arabidopsis

Zhenbiao Yang (yang@ucr.edu)
University of California, Riverside https://orcid.org/0000-0001-7482-6540

Wenwei Lin
University of California, Riverside

Wenxin Tang
FAFU-UCR Joint Center for Horticultural Biology and Metabolomics, Haixia Institute of Science and Technology, Fujian Agriculture and Forestry University

Koji Takahashi
Graduate School of Science, Nagoya University https://orcid.org/0000-0001-5438-7624

Hong Ren
University of Minnesota

Songqin Pan
University of California, Riverside

Haiyan Zheng
Biological Mass Spectometry Facility, RWJMS, Rutgers University https://orcid.org/0000-0003-1955-1817

William Gray
University of Minnesota

Tongda Xu
Fujian Agricultural and Forestry University https://orcid.org/0000-0003-3398-9217

Toshinori Kinoshita
Nagoya University https://orcid.org/0000-0001-7621-1259

Biological Sciences - Article

Keywords: auxin signaling, plants, cell expansion

Posted Date: February 15th, 2021

DOI: https://doi.org/10.21203/rs.3.rs-203621/v1

Version of Record: A version of this preprint was published at Nature on October 27th, 2021. See the published version at https://doi.org/10.1038/s41586-021-03976-4.

TMK-based cell surface auxin signaling activates cell wall acidification in Arabidopsis

Wenwei Lin[1,2], Wenxin Tang[1], Koji Takahashi[3,4], Hong Ren [5], Songqin Pan[2], Haiyan Zheng[6], William M. Gray[5], Tongda Xu[1], Toshinori Kinoshita[3,4], and Zhenbiao Yang[2]

[1]FAFU-UCR Joint Center for Horticultural Biology and Metabolomics, Haixia Institute of Science and Technology, Fujian Agriculture and Forestry University, Fuzhou, Fujian, China

[2]Institute of Integrative Genome Biology and Department of Botany and Plant Science, University of California, Riverside, CA, USA

[3]Graduate School of Science, Nagoya University, Nagoya, Japan

[4]Institute of Transformative Bio-Molecules, Nagoya University, Nagoya, Japan

[5]Department of Plant and Microbial Biology, University of Minnesota, St. Paul, MN, USA

[6]Biological Mass Spectrometry Facility, Robert Wood Johnson Medical School and Rutgers, the State University of New Jersey, Piscataway, NJ, USA

*Correspondence to: yang@ucr.edu

Abstract

The phytohormone auxin controls a myriad of processes in plants, at least in part through its regulation of cell expansion. The "acid growth hypothesis" has been proposed to explain auxin-stimulated cell expansion for five decades, but the mechanism underlying auxin-induced cell wall acidification is poorly characterized. Auxin induces the phosphorylation and activation of the plasma membrane (PM) H^+-ATPase that pumps protons into the apoplast, yet how auxin activates its phosphorylation remains elusive. Here, we show that the transmembrane kinase (TMK) auxin signaling proteins interact with PM H^+-ATPases and activate their phosphorylation to promote cell wall acidification and hypocotyl cell elongation in *Arabidopsis*. Auxin induced TMK's interaction with H+-ATPase on the plasma membrane within 1-2 minutes as well as TMK-dependent phosphorylation of the penultimate Thr residue. Genetic, biochemical, and molecular evidence demonstrates that TMKs directly phosphorylate PM H^+-ATPase and are required for auxin-induced PM H^+-ATPase activation, apoplastic acidification, and cell expansion. Thus, our findings reveal a crucial connection between auxin and PM H^+-ATPase activation in regulating apoplastic pH changes and cell expansion via TMK-based cell surface auxin signaling.

One Sentence Summary: TMK-based cell surface auxin signaling directly activates the phosphorylation of the plasma membrane H^+-ATPase, leading to H^+ pump activation, cell wall acidification, and cell elongation in Arabidopsis hypocotyls.

Main

Embedded in a rigid cell wall, the plant cell must modify its wall to gain the adjustable elasticity to regulate cell expansion in space and time. Auxin induces rapid cell expansion by acidifying the cell wall space (apoplast), leading to the activation of cell wall-localized proteins for wall loosening [1,2], a growth mechanism that has been

known as the acid-growth theory for half of a century [3]. Auxin triggers the efflux of protons resulting in apoplastic acidification by activating the plasma membrane (PM) localized P-type H^+-ATPase[4,5]. In Arabidopsis, PM H^+-ATPase is encoded by an *AHA* (Autoinhibited, H^+-ATPase) gene family with 11 members [6]. Phosphorylation of the conserved penultimate Thr residue (Thr-948 in AHA1, Thr-947 in AHA2) has been proposed to release the autoinhibition of the ATPase pump activity by the cytoplasmic C-terminal region[7,8,9-13]. Recently, Fendrych et al. demonstrated that auxin-induced apoplastic acidification and growth were mediated by TIR1/AFB-Aux/IAA nuclear auxin perception in hypocotyls[14]. Auxin induces the TIR1/AFB-dependent expression of SAUR proteins that act as an inhibitors of PP2C.D phosphatases, which dephosphorylate the penultimate Thr[15]. While this mechanism can sustain H^+-ATPase activity by preventing penultimate Thr dephosphorylation, it cannot account for how the PM H^+-ATPase is initially phosphorylated to become activated.

The PM-localized TMK receptor-like kinases play a vital role in auxin signaling in regulating pavement cell morphogenesis, differential growth of the apical hook, and lateral root (LR) formation in *Arabidopsis* [16-20]. Auxin rapidly promotes TMK-dependent activation of PM-associated ROP GTPases within seconds, providing a mechanism for rapid auxin responses on the cell surface in addition to TIR1/AFB-based intracellular auxin signaling [18,21]. To identify new components in TMK-mediated auxin signaling pathways, we performed immunoprecipitation coupled with mass spectrometry (IP-MS) to isolate potential interactors of TMK1 in *Arabidopsis*. Briefly, GFP-trap agarose beads were used to immunoprecipitate the TMK1-GFP protein complex from *pTMK1::TMK1-GFP* transgenic plants, which was further analyzed by MS. The proteins that were identified only from the *pTMK1::TMK1-GFP* transgenic plants but not from *pTMK1::GFP* control plants were considered as candidates for TMK1-associated proteins. Among them, we were especially interested in the PM H^+-ATPases (AHAs) (Fig1. a), as the previous study showed that auxin triggers the activation of the PM H^+-ATPase, which promotes hypocotyl cell elongation[22]. We further confirmed that GFP-AHA1 immunoprecipitated TMK1 and

TMK4 in the *35S::GFP-AHA1* transgenic plants as detected by immunoblot with α-TMK1 and α-TMK4 antibodies, respectively (Fig. 1b, Extended Data Fig. 1a). Furthermore, TMK1-GFP immunoprecipitated AHA(s) from *pTMK1::TMK1-GFP* transgenic plants as detected by immunoblot analysis with an α-AHA2-cat antibody upon an α-GFP-trap antibody immunoprecipitation (Extended Data Fig.1b). *In vitro* pull-down assay showed the kinase domain of TMK1 (TMK1KD), when fused to maltose-binding protein (MBP), directly interacted with the AHA2 C-terminal domain fused to glutathione S-transferase (GST) (GST-AHA2-C) (Extended Data Fig. 1c), suggesting that the kinase domain of TMK1 directly binds the C-terminal region of AHA2. We postulated that TMK1 interacts with AHAs *in vivo* since both proteins are predominantly localized on the PM[18,23,24]. We used fluorescence resonance energy transfer (FRET) analysis to test this hypothesis. Due to the poor expression of TMK1 in *Nicotiana benthamiana*, we expressed a kinase-dead form of TMK1 (TMK1K616E). As shown in Fig 1c, strong FRET signals were detected on the PM in the cells co-expressing AHA1-YFP with TMK1Km-CFP but not with TMK1ext-CFP (the extracellular domain of TMK fused with CFP), confirming that TMK1 directly interacts with AHA1 *in vivo* (Fig. 1c). This result also suggested that the kinase activity of TMK1 is not a prerequisite for the interaction with AHA *in vivo*. To investigate the relevance of auxin in the TMK1-AHA interaction, we performed a coimmunoprecipitation (Co-IP) assay using protoplasts co-expressing Myc epitope-tagged TMK1 and HA epitope-tagged AHA1. As shown in Fig. 1d, the *in vivo* association of TMK1 with AHA1 was enhanced within 1 minute upon NAA treatment (Fig. 1d), suggesting that auxin rapidly promotes TMK1-AHA interactions.

a

Identified Proteins	Accession	Unique peptide
H(+)-ATPase 1 AHA1	AT2G18960	14
H(+)-ATPase 2 AHA2	AT4G30190	19
H(+)-ATPase 3 AHA3	AT5G57350	3
H(+)-ATPase 7 AHA7	AT3G60330	1
H(+)-ATPase 11 AHA11	AT5G62670	18

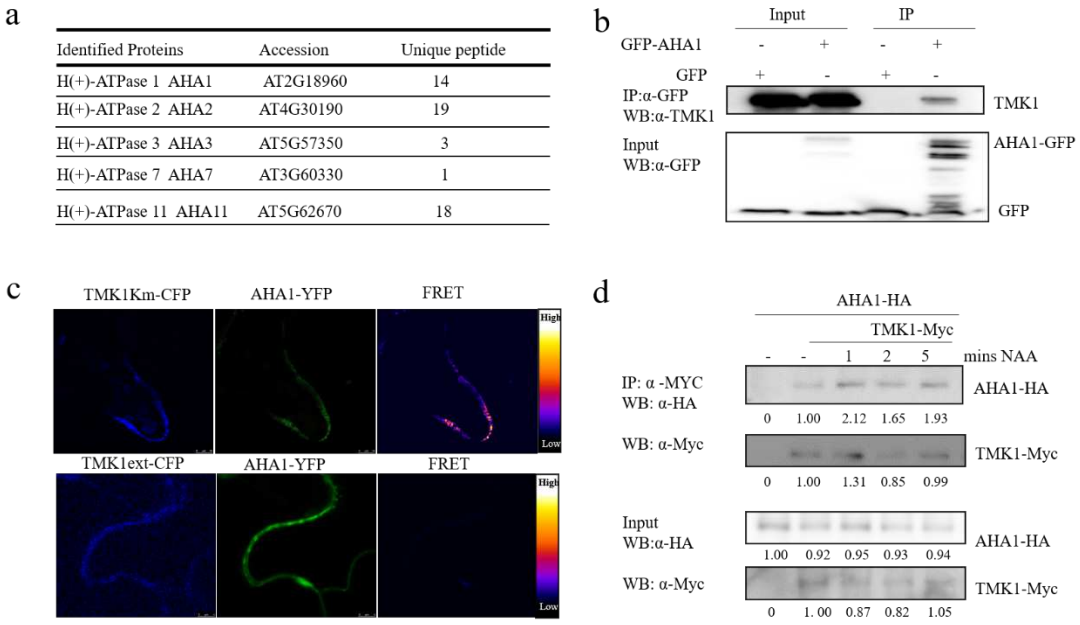

Fig. 1. TMK1 directly interacts with AHAs. a, Summary of LC-MS/MS analysis of AHAs associated with TMK1-GFP. The number of unique AHA peptides identified in the immunoprecipitates from *pTMK1::TMK1-GFP* transgenic seedlings is shown. IP-MS did not identify any AHA peptides from control *pTMK1::GFP* seedlings. **b**, co-immunoprecipitation of TMK1 with AHA1 in transgenic plants. Membrane proteins from 4-week-old *35S::GFP and 35S::GFP-AHA1* plants were immunoprecipitated with α-GFP-Trap antibody and analyzed with Western blotting using an α-TMK1 antibody (Top). The expression of AHA1-GFP and GFP control in transgenic plants is shown in the bottom panel. The experiments were repeated three times with similar results. **c**, TMK1 interacted with AHA1 on the PM. FRET analysis in *Nicotiana benthamiana* leaf epidermal cells transiently co-expressing TMK1Km-CFP and AHA1-YFP showed TMK1Km-CFP directly interacted with AHA1-YFP on the PM. The transient expression was achieved by agrobacterium infiltration. The extracellular domain of TMK1 (TMK1ext-CFP) did not interact with AHA1-YFP in *N. benthamiana*. More than 10 cells were determined with similar results. **d**, TMK1's association with AHA1 in Arabidopsis protoplasts was rapidly enhanced by auxin treatments within 1 minute. TMK1-Myc was co-expressed with AHA1-HA in Arabidopsis protoplasts. Co-IP was carried out with an α-Myc antibody (IP: α-Myc), and the proteins were analyzed by using Western blot with an α-HA antibody. Top shows that AHA1-HA coimmunoprecipitated with TMK1-Myc (IP: α-Myc; WB: α-HA, WB: α-Myc). The Middle and Bottom show the expression of AHA1-HA and TMK1-Myc proteins, respectively (WB: α-HA or α-Myc for input control). Protoplasts were treated with 1 μM NAA for 1, 2, and 5 minutes as indicated. The number under the immunoblot is the relative signal intensities as determined by ImageJ. Similar results were reproduced twice in experiments involving 2 min and 5 min NAA treatments.

The penultimate threonine (Thr) residue of the H^+-ATPase protein is conserved among the AHA family members, and the phosphorylation of this residue is a primary mechanism by which the H^+-ATPase is activated in response to multiple signals,

including phytohormones, sucrose, NaCl, blue light, and the fungal toxin fusicoccin[11,12,22,25-27]. Thus, we tested whether auxin activates AHA phosphorylation through TMKs. We examined the phosphorylation status of the penultimate Thr of the H^+-ATPase in the aerial parts of Arabidopsis seedlings by phosphoproteomics. The phosphorylation levels of the penultimate Thr of AHA1, AHA2, and AHA11 were compromised in the *tmk1-1 tmk4-1* mutant compared to wild type (Extended Data Fig. 2a), implying a general reduction of H^+-ATPase activity in the mutant. TMK1 and TMK4 are functionally redundant in the regulation of Arabidopsis seedling growth, as neither of *tmk1* and *tmk4* single knockout mutants exhibits a visible growth defect, while *tmk1 tmk4* double mutants show severe growth retardation, especially in hypocotyl elongation [23] (also see below).

To further investigate the role of TMK1 and TMK4 in auxin-induced PM H^+-ATPase activation, we analyzed the phosphorylation status of the penultimate Thr residue by immunoblot analysis using anti-pThr-947 antibody, which recognizes the unique phosphorylation of the penultimate Thr in all of the AHA isoforms[22]. Fusicoccin (FC) promotes the binding of 14-3-3 to the phosphorylated C-terminal region of PM H^+-ATPase, resulting in the pump activation. As shown previously[12], FC increased the level of penultimate Thr phosphorylation in wild type Col-0 seedlings (Fig. 2a, b). Similarly, auxin treatment greatly increased its phosphorylation level (Fig. 2a, b). Compared with untreated wild type, the level of phosphorylated penultimate Thr was reduced in the *tmk1-1 tmk4-1* mutant (Fig. 2.a, b). Importantly, auxin-induced phosphorylation of this residue was dramatically reduced in the *tmk1-1 tmk4-1* mutant (Fig. 2a,b). Thus, TMK1 and TMK4 are required for the auxin-induced increase in penultimate Thr phosphorylation. We were unable to assess whether TMKs directly phosphorylate AHA at this penultimate Thr residue using AHA1-C terminal recombinant proteins purified from *E. coli*, because we did not detect a TMK-induced increase in the phosphorylated T947 residue using the anti-pThr-947 antibody possibly due to its phosphorylation prior to the addition of TMKs. Thus, we immunoprecipitated AHA1-GFP from Arabidopsis protoplasts that transiently

expressed this fusion protein for *in vitro* phosphorylation assay. Recombinant TMK1KD, but not kinase-dead (TMK1KDKm), greatly increased the phosphorylation of AHA1-GFP on the T948 (T947 of AHA2) residue *in vitro* (Fig. 2c). We further determined whether TMK1 phosphorylated a synthetic peptide containing the C-terminal 16 amino acid residues from AHA1 (AHA1-C16) in an *in vitro* phosphorylation assay. Mass spectrometry analysis showed that the penultimate Thr residue (T15 of the peptide, T948 of AHA1) of the AHA1-C16 peptide was highly phosphorylated by the recombinant TMK1KD, but not by TMK1KDKm (Fig. 2d, Extended Data Fig. 2b). The second to the last Thr residue (T9T15) of the AHA1-C16 peptide was weakly phosphorylated by TMK1KD. Neither TMK1KD nor TMK1KDKm phosphorylated the scrambled synthetic peptide (Fig. 2d). Thus, TMK1 specifically phosphorylates the penultimate Thr residue of AHA1. Together with auxin-induced rapid interaction of TMK1 with AHA1 and the requirement of TMK1 and TMK4 for auxin-induced AHA phosphorylation *in vivo*, these results strongly indicate a role for TMK1 in the direct phosphorylation of AHA1 activated by auxin.

We next investigated whether TMK1 and TMK4 are required for the activation of PM H^+-ATPase by auxin. The activation of PM H^+-ATPase couples with the ATP hydrolysis[12]. As shown previously[22], auxin treatment for 30 minutes increased ATP hydrolysis in the aerial parts of wild type Arabidopsis seedlings (Fig. 2e). Neither *tmk1-1* nor *tmk4-1* mutations significantly affected auxin-induced changes in ATP hydrolysis. In contrast, auxin-induced enhancement of ATP hydrolysis was abolished in the *tmk1-1 tmk4-1* mutant (Fig. 2e), indicating that TMK1 and TMK4 are essential for auxin-induced H^+-ATPase activation. In agreement with the compromised H^+-ATPase activity in the *tmk1-1 tmk4-1* mutant, we found that the *tmk1-1 tmk4-1* mutant was more tolerant to lithium than the wild type (Extended Data Fig. 2c, d), a toxic alkali cation, whose uptake is coupled with the activation of H^+-ATPase and hyperpolarized PM. In particular, the aerial part of wild type seedlings became chlorotic but *tmk1-1 tmk4-1* remained green after growth on lithium. This is in contrast to SAUR19-OX lines, which display increased H^+-ATPase activity and thus

exhibit much higher sensitivity to lithium[15]. These findings together demonstrate that TMK1 and TMK4 are required for auxin-induced PM H$^+$-ATPase activation.

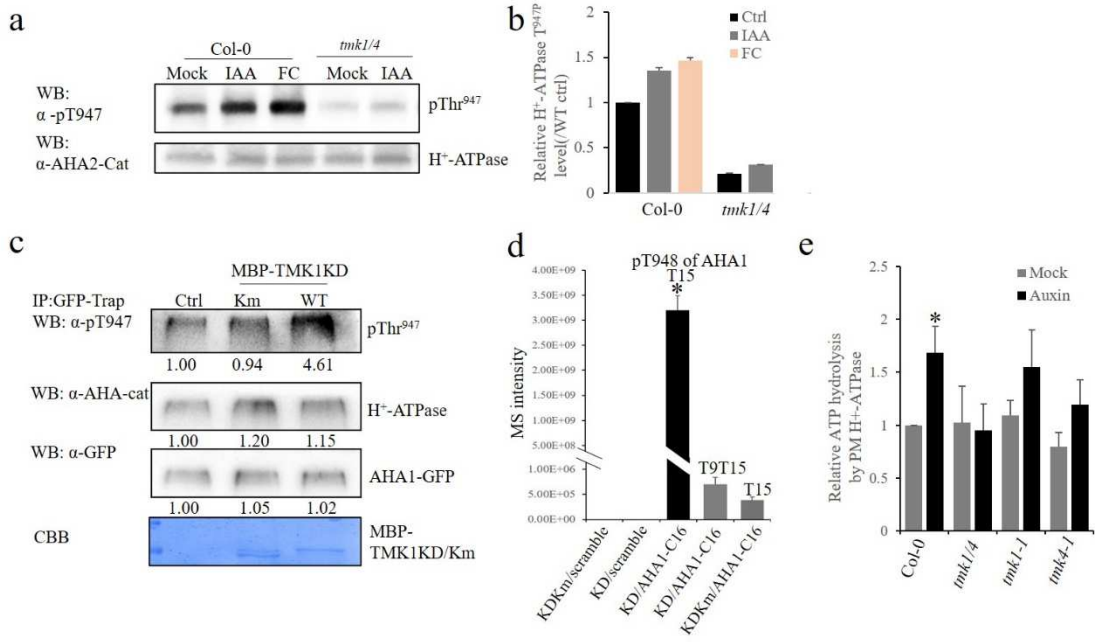

Fig. 2. **TMK1 and TMK4 are required for auxin-induced phosphorylation and activation of the PM H$^+$-ATPase**. **a**, Auxin-induced AHA phosphorylation is compromised in the *tmk1-1 tmk4-1*(*tmk1/4*) mutant. The endogenous auxin-depleted aerial sections of seedlings were incubated with 100 nM IAA for 10 minutes or 10 μm fusicoccin (FC) for 5 minutes, respectively. The amounts of H$^+$-ATPase and the phosphorylation status of the penultimate Thr in the C terminus were determined by immunoblot analysis with anti-H$^+$-ATPase (H$^+$-ATPase) and anti-pThr-947 (pThr 947) antibodies, respectively. **b**, Quantification of the phosphorylation level of the H$^+$-ATPase. Values are means ± SD; n = 3 independent experiments. **c**, MBP-TMK1KD phosphorylated AHA1-GFP *in vitro*. AHA1-GFP was transiently expressed in Arabidopsis protoplasts and immunoprecipitated by GFP-trap. The GFP-trap beads immobilized AHA1-GFP proteins were incubated with TMK1 (TMK1KD, WT) or kinase-dead form (TMK1KD,Km) for 1 hr. The amounts of H$^+$-ATPase and phosphorylated penultimate Thr were determined by immunoblot analysis with anti-H$^+$-ATPase (H$^+$-ATPase) and anti-pThr-947 (pThr 947) antibodies, respectively. The AHA1-GFP proteins were determined by immunoblot analysis with an anti-GFP antibody. The input MBP-TMK1KD and MBP-TMK1KDKm recombinant proteins were detected by coomassie brilliant blue staining (CBB). The number under the immunoblot is the relative signal intensities as determined by ImageJ. **d**, MBP-TMK1KD phosphorylated the synthetic AHA1-C16 peptide *in vitro*. MBP-TMK1KD or MBP-TMK1KDKm (1 μg) was incubated with the AHA1-C terminal synthetic peptide (KLKGLDIDTAGHHITV) or a scrambled peptide (GDAHVKITHLDKGLIT) (10 μg) in 100 μl phosphorylation buffer, respectively. The peptides were then analyzed by mass spectrometry. The graph shows the abundance of phosphorylated peptides at the indicated residues analyzed mass spectrometry. Values are means ±SD; n =3. * P ≤ 0.01, results of One-way ANOVA-tests. Two biological replicates with three technical replicates/each produced similar results. **e**, Auxin induction of H$^+$-ATPase activity in the aerial

parts of wild type and the *tmk1-1 tmk4-1* mutant. Aerial sections of 14-days old seedlings were treated with 10 μm IAA for 30 minutes and used for vanadate-sensitive ATP hydrolysis assay by determining the inorganic phosphate released from ATP as described previously [25]. The values shown are relative ATP hydrolytic activity of indicated samples to that of control Col-0 without auxin treatment. Values are means ± SD; n =3. * P $\leqslant$ 0.05, results of paired Student's t-tests.

To assess the consequence of the reduction of PM H^+-ATPase activity in *tmk1-1 tmk4-1*, we introduced membrane-impermeable 8-hydroxypyrene-1,3,6-trisulfonic acid trisodium salt (HPTS) as a ratiometric fluorescent pH indicator for assessing changes in the apoplastic pH at the cellular resolution in *Arabidopsis thaliana* hypocotyls [2]. Two different forms of HPTS (the protonated and deprotonated) were visualized in 2 independent channels with excitation wavelengths of 405 and 458 nm, respectively. The apoplastic pH correlates with the ratiometric values (signal intensity from the 458-nm channel divided by that from the 405-nm channel) [2,28]. As a positive control for the HPTS-based pH indicator, we monitored the apoplastic pH in hypocotyls of the *ost2-2D* mutant harboring the constitutively activated PM H^+-ATPase AHA1[29]. As shown previously [2], the *ost2-2D* mutant exhibited lower 458/405 values compared with the wild type (Fig. 3a, b), confirming the apoplastic acidification in the *ost2-2D* mutant. In contrast, significantly higher 458/405 values were observed in *tmk1-1 tmk4-1* hypocotyls, suggesting apoplastic alkalization in the mutant (Fig. 3a, b). Furthermore, the apoplastic pH of the *tmk1-1 tmk4-1* mutant was restored to the wild type level when this mutant was complemented with wild type TMK1 (Extended Data Fig. 3a,b), indicating that TMK1 is essential for the regulation of the apoplastic pH.

Importantly, we found that hypocotyl cell length was correlated with the pH value of the mutant when compared to the wild type (Fig. 3c). In *tmk1-1 tmk4-1*, the mean length of hypocotyl cells was significantly shorter than in wild type (Fig. 3a, and Fig. 3c) [23]. In contrast, increased apoplastic acidification is linked to an increase in cell length and hypocotyl length in *ost2-2D (*Fig.3a, and Extended Data Fig. 3c and d*)*.

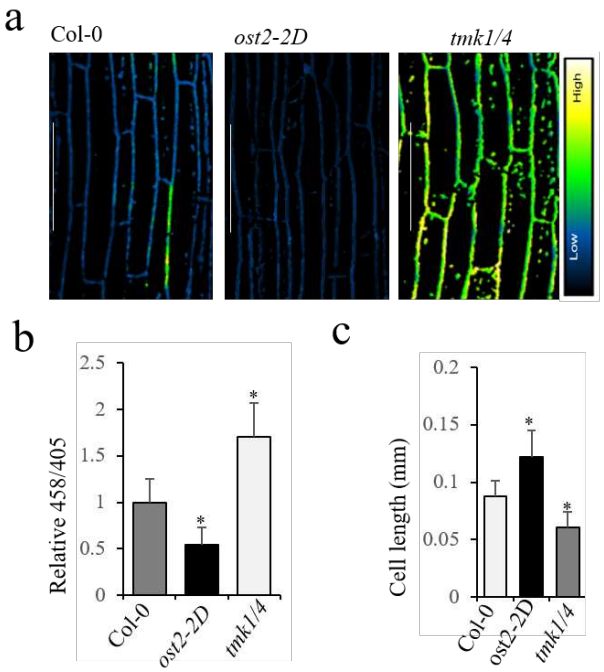

Fig. 3. TMK1 and TMK4 are required for apoplastic acidification and cell elongation in Arabidopsis hypocotyl. a and **b,** Comparison of the apoplastic pH in wild type (Col-0), *ost2-2D,* and the *tmk1-1 tmk4-1* (*tmk1/4*) mutant. Changes in pH were visualized with ratiometric values of fluorescent HPTS. Y-Axis: the mean 458/405 values of *ost2-2D* and the *tmk1-1 tmk4-1* mutant relative to the WT. **c**, Epidermal cell lengths of hypocotyls from two days-old etiolated seedlings were measured using Image J. Hypocotyl epidermal cells in the 100-500 μM region after apical hook were measured. Values are means ±SD; (n>20 cells per line). * P⩽0.05. Scale bar=100 μM

Auxin promotes the acidification of the apoplast in hypocotyls via the activation of PM H^+-ATPase, contributing to auxin-induced cell elongation [14,22]. We found that the auxin-induced acidification in the apoplast was completely abolished in the *tmk1-1 tmk4-1* mutant (Fig. 4a, b), suggesting an essential role of TMK1 and TMK4 in auxin-triggered PM H^+-ATPase activation. Moreover, exogenous NAA promoted the elongation of auxin-depleted hypocotyl segments in wild type, but not in the *tmk1-1 tmk4-1* mutant (Fig. 4c). The *tmk1-1 tmk4-1* mutant complemented with TMK1 exhibited a normal response to auxin in promoting hypocotyl segment elongation (Fig. 4c). The severe defect in *tmk1-1 tmk4-1* hypocotyl elongation was partially rescued when *tmk1-1 tmk4-1* seedlings were grown on the medium with lower pH (pH 5.0 and pH 4.3) compared to standard medium (pH 5.7) (Extended Data Fig. 4a,b). Moreover, *ost2-2D,* which caused activation of the PM H^+-ATPase, partially rescued

the hypocotyl elongation defect of *tmk1-1 tmk4-1* (Extended Data Fig. 4c,d). TMK1 and TMK4 likely activate other downstream pathways to regulate hypocotyl elongation in addition to the PM H^+-ATPase activation, such as ROP GTPase signaling to the organization of the cytokseleton[18,30]. Such additional downstream pathways may explain the incomplete rescue of the hypocotyl elongation defect in *tmk1-1 tmk4-1* by *ost2-2D*. Taken together, our results indicate that TMK1 and TMK4 are required for apoplastic acidification via the auxin-triggered PM H^+-ATPase activation, contributing to auxin regulation of hypocotyl cell elongation.

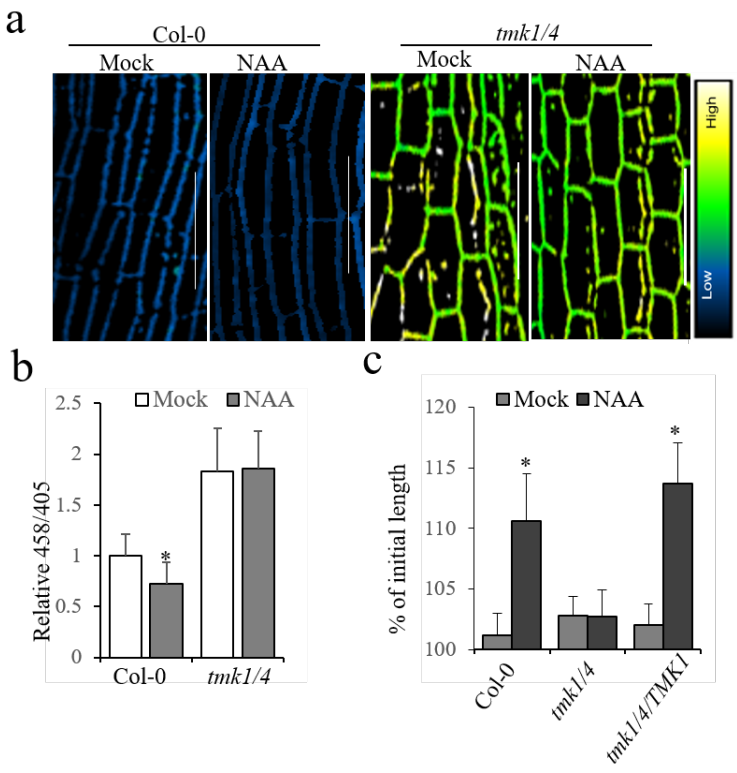

Fig. 4. TMK1 and TMK4 are required for auxin-induced apoplastic acidification and hypocotyl elongation. a, and **b,** The *tmk1-1 tmk4-1* (*tmk1/4)* mutant is insensitive to auxin-induced apoplastic pH changes. Effect of auxin on the apoplastic change as visualized by HPTS staining. 2-day etiolated seedlings were treated with 100 nM NAA for 15 minutes. Error bar represents SEM (n>10 hypocotyls per line). **c**, Auxin-induced hypocotyl elongation was compromised in the *tmk1-1 tmk4-1* (*tmk1/4*) mutant. The auxin-depleted hypocotyl sections were treated with/without 10 μM NAA for 30 minutes. The hypocotyl sections were measured by Image J at 0 and 30 minutes after treatments. The Y-axis represents the relative length when comparing the hypocotyl segments at 30 minutes to that at 0 minute. TMK1 restored the defect of auxin-induced hypocotyl elongation in the *tmk1-1 tmk4-1* mutant (*tmk1/4 TMK1*). Values are

means ±SD; Error bar represents SD (n>20 hypocotyl sections per line), * P ⩽ 0.05. Scale bar= 100 μM.

In this work, we showed that TMK1 directly interacts with PM H^+-ATPases on the PM, and this interaction was induced rapidly (within 1-2 min) by auxin treatment (Fig.1d), preceding an anxin-induced increase in cell elongation[14]. Therefore, the auxin-induced TMK-AHA association can be considered as the very early response for auxin signal transduction. Once interacting with AHAs upon auxin stimulation, TMK1 directly phosphorylates AHA1 on the penultimate Thr residue (Fig. 2c, d). Furthermore, auxin induced the phosphorylation of AHA's penultimate Thr in a TMK1/TMK4-dependent manner (Fig.2 a, b, and Extended Data Fig. 2a). This auxin-induced phosphorylation of AHA's penultimate Thr occurred in root tissues within 2 minutes after auxin treatment (Li et al. accompanying manuscript), nearly as rapid as the auxin-induced interaction between TMK1 and AHA1 (Fig.1d). Therefore, TMK regulates AHA activation by directly affecting the phosphorylation status of the penultimate Thr. Consequently, auxin induced apoplastic acidification in a TMK1/TMK4-dependent manner in hypocotyl cells (Fig. 3a, b, and Fig. 4a,b). Moreover, reducing the apoplast pH either genetically by *ost2-2D* or growing seedlings in an acidic environment partially restored the hypocotyl elongation defect of *tmk1-1 tmk4-1* (Extended Data Fig. 4a-d). These data shows that the cell surface auxin signaling component TMKs act as a protein kinase that responds to auxin to rapidly and directly initiate the phosphorylation of PM H^+-ATPases, triggering their activation and apoplastic acidification, and thereby promoting cell expansion. In contrast, the TIR1/AFB-dependent nuclear auxin signaling pathway activates the expression of SAUR proteins that inhibit the PP2C.D-mediated dephosphorylation and inactivation of PM H^+-ATPase[15,31,32]. The mechanism for the perception of auxin that activates the TMK-based cell surface signaling remains to be determined. Nonetheless, the current findings strongly support the hypothesis that the cell surface and intracellular auxin signaling pathways respectively initiate and sustain PM H^+-ATPase activation in cells where auxin promotes cell expansion, such as in hypocotyls, and collectively explain the acid growth theory. In roots, TMK-dependent

auxin signaling also promotes ATPase activation, but to counter the rapid alkalization (or membrane depolarization) activated by TIR1/AFBs[33,34] (Li et al. accompanying manuscript). Importantly, these findings, together with the recent findings on the TMK-mediated noncanonical auxin signaling in regulating pavement cell morphogenesis[18,35] (Perez et al. manuscript in preparation), differential growth of the apical hook[16], LRs formation[17], and root gravitropic response[36] are emerging as a common theme that auxin regulates growth and developmental processes via the coordinate actions of intracellular and cell surface auxin signaling systems.

Materials and Methods

Plant materials and growth conditions. Columbia Col-0 was used as wild type in this study. *ost2-2D* seeds were obtained from Jeffrey Leung (Department of Institut Jean-Pierre Bourgin, INRA, Versailles, France). The *tmk1-1 tmk4-1* mutant and *pTMK1-TMK1-GFP* transgenic lines (generated in the *tmk1-1 tmk4-1* background) were described previously [16,17]. The *ost2-2D tmk1-1 tmk4-1* mutants were generated by genetic crosses and confirmed by genotyping. *Arabidopsis* plants were grown in soil (Sungro S16-281) in a growth room at 23 °C, 40% relative humidity, and 75 μE m-2·s-1 light with a 12-h photoperiod for approximate 4 weeks before protoplast isolations. To grow *Arabidopsis* seedlings, the seeds were surface sterilized with 50% bleach for 10 minutes (for *tmk1-1tmk4-1* seeds were sterilized with 75% (vol/vol) ethanol for 5 minutes), and washed 3 times with sterilized distilled H_2O, and then placed on the plates with 1/2 MS medium containing 0.5% sucrose and 0.8% agar at pH 5.7 at dark with vertical growth. 2 to 3 days after germination (DAG) hypocotyls were used for cell characterization.

Plasmid construction and generation of transgenic plants. Full-length and truncated variants *TMK1*, *AHA1,* and *AHA2* were amplified by PCR from Col-0 cDNA and cloned into a protoplast transient expression vector (HBT vectors obtained from Libo Shan & Ping He, Texas A&M) or plant expression vector pGWB641 and pGWB644 Stable transgenic lines were generated by using the standard

Agrobacterium tumefaciens-mediated transformation in the *tmk1-1 tmk4-1* mutant or Col-0 [37]. AHA2-C terminal region was cloned into pDest-565, and expressed in *E.coli* (Rosetta, BL21).

Determination of H^+-ATPase phosphorylation levels. The immunoblot was performed as described by Hayashi[38] by using specific antibodies against the catalytic domain of AHA2 and phosphorylated Thr-947 in AHA2[39]. These antibodies recognize not only AHA2 but also other H^+-ATPase isoforms in Arabidopsis[39]. Briefly, ten pieces of auxin-depleted aerial sections were collected and grounded with a plastic pestle, followed by solubilization in 40 μL of SDS buffer (3% [w/v] SDS, 30 mM Tris-HCl [pH 8.0], 10 mM EDTA, 10 mM NaF, 30% [w/v] Sucrose, 0.012% [w/v] Coomassie Brilliant Blue, and 15% [v/v] 2-mercaptoethanol), and the homogenates were centrifuged at room temperature (10,000g for 5 min). 12 μL of the supernatant was loaded onto 10% (w/v) SDS PAGE gels to assess the H^+-ATPase or the phosphorylated penultimate Thr levels by using the above-mentioned antibodies, respectively. A goat anti-rabbit IgG conjugated to horseradish peroxidase (Santa Cruz) was used as a secondary antibody. The chemiluminescent signal was quantified using ImageJ software.

HPTS staining and imaging. HPTS staining and imaging were performed as described by Barbez [2] with modification. Briefly, 2-day etiolated seedlings were transferred and incubated with 1 mM HPTS (from 100 mM water stock) with 0.01% Triton-X-100 under vacuum (10-15 pa) 5 minutes. The seedlings were then incubated with HPTS for 60 minutes in the liquid growth medium. The seedlings were subsequently mounted in the same growth medium on a microcopy slide and covered with a coverslip. For auxin treatment, seedlings were incubated in 1/2 MS growth medium supplemented with 1 mM HPTS and NAA in the stated concentration and subsequently mounted in the same growth medium on a microcopy slide and covered with a coverslip. Seedling imaging was performed using an inverted Zeiss 880 confocal microscope equipped with a highly sensitive GaAsP detector. Fluorescent signals for the protonated HPTS form (Excitation 405 nm, emission peak 514nm), as

well as the deprotonated HPTS form (excitation, 458 nm emission peak, 514 nm), were detected with a 10× (water immersion) objective.

Immunoprecipitation-mass spectrometry analyses. One gram of *pTMK1-gTMK1-GFP/tmk1-1 tmk4-1* seedlings grown on 1/2 MS medium was collected and grounded in liquid nitrogen with a mortar and pestle. Total proteins were extracted by extraction buffer (50 mM Tri-HCl pH 7.4, 150 mM NaCl, 5 mM EDTA, 0.5% Triton X-100 with protease inhibitor and phosphatase inhibitor) on ice. The extracts were centrifugated at 13,000g for 30 min, and the supernatants were incubated with GFP-trap agarose beads (GFP-Trap®_A, gta-20, ChromoTek) at 4 ℃ for 2 hours to immunoprecipitate TMK1-GFP proteins. The agarose beads were washed and resuspended with 50 mM Tris-Cl buffer (pH7.8). One 10^{th} of the beads were used for immunoblot analysis with an anti-GFP antibody. The remaining agarose beads were used for LC-MS/MS analysis. MS analysis was carried out by Orbitrap Fusion mass spectrometry (Thermo Fisher Scientific, Waltham, MA).

Phosphoproteomics Analyses. Col-0 and the *tmk1-1 tmk4-1* seedlings were cultured on ½ MS plate for 5 days, then the aerial parts of seedlings were transferred to ½ MS liquid medium and incubated in KPSC buffer (10 mM potassium phosphate, pH 6.0, 2% sucrose, 50 μm chloramphenicol) in darkness overnight, and the buffer was replaced every 1 hr for 12 hrs [40]. Seedings were collected and flash-frozen in liquid nitrogen. A total of 1 g of frozen shoots (fresh weight) was grounded with liquid nitrogen pre-cold mortar and homogenized in 5 ml extraction buffer [50 mM Tris-HCl buffer (pH 8), 0.1 M KCl, 30% sucrose, 5 mM EDTA, and 1 mM DTT in Milli-Q water, 1x complete protease inhibitor mixture and the PhosSTOP phosphatase inhibitor mixture] in a Dounce Homogenizer. At least 50 strokes were performed. The homogenate was filtered through four layers of miracloth and centrifuged at 5000 × *g* at 4◦C for 10 min. Half of the supernatant was used to resuspend the pellet, and the mixture was centrifuged again at 5000g 4◦C for 10 min. The two fractions of the supernatants were combined and mixed with 3, 1, and 4 volumes of methanol, chloroform, and water, respectively. The mixtures were centrifuged at 5000 × *g* for 10

min, and the aqueous phase was removed. After the addition of 4 volumes of methanol, the proteins were pelleted via centrifugation at 4000 × *g* for 10 min. Pellets were washed with 80% acetone and resuspended in 6 M guanidinium hydrochloride in 50 mM triethylammonium bicarbonate (TEAB) buffer (pH 8). The proteins were used for Tandem Mass Tag（TMT）labeling according to the Kit protocol (Thermo Scientific #90096) and quantitation by mass spectrometry (MS).

Protoplast preparation and transient expression. Protoplasts were prepared according to the protocol described by Yoo et al[41].Maxiprep DNA for transient expression was prepared using the Invitrogen PureLink Plasmid Maxiprep Kit. $2x10^5$ protoplasts were transfected with indicated AHA1-HA or TMK1-myc and incubated at room temperature for 10 hours. The protoplasts were collected and stored at -80 °C for further usage.

Coimmunoprecipitation (Co-IP) assay. 2×10^5 protoplasts were transfected with indicated plasmids and incubated for 7-10 hours at room temperature. Protoplasts were then collected in 2 ml Eppendorf tubes and subjected to centrifuge with a swinging-basket centrifuge at 100 x *g* for 1 minute. The supernatant was discarded, and the protoplasts were resuspended with 100 μl W5 solution (2 mM MES-KOH, pH 5.7, 5 mM KCl, 154 mM NaCl, and 125 mM $CaCl_2$). The protoplasts were treated with 1 μM NAA for the indicated time period, frozen in liquid N_2 immediately and stored in -80 ºC. The samples were lysed with 0.5 mL of extraction buffer (10 mM HEPES at pH 7.5, 100 mM NaCl, 1 mM EDTA, 10% (vol/vol) glycerol, 0.5% Triton X-100, and protease inhibitor mixture from Roche). After vortexing vigorously for 30 s, the samples were centrifuged at 12,470 × g for 10 min at 4 °C. The supernatant was incubated with an anti-GFP-Trap antibody for 2 h with gentle shaking. The beads were collected and washed three times with washing buffer (10 mM HEPES at pH 7.5, 100 mM NaCl, 1 mM EDTA, 10% glycerol, and 0.1%Triton X-100) and once with 50 mM Tris·HCl at pH 7.5. The immunoprecipitated proteins were analyzed by immunoblot with α-GFP or α-HA antibody. For seedling Co-IP, approximate 1 g of

10-day old seedlings were grounded in liquid N_2 and further grounded in 0.5 mL of ice-cold Co-IP buffer (10 mM HEPES at pH 7.5, 100 mM NaCl, 1 mM EDTA, 10% glycerol, and 0.1%Triton X-100, and protease inhibitor mixture from Roche). The homogenates were centrifuged at 12,470 × g at 4 °C for 10 min. The resulting supernatants were used to perform the Co-IP assay with the same procedures as protoplast Co-IP assay with α-GFP-Trap antibodies.

***In vitro* pull-down assay**.

MBP or GST fusion proteins were expressed in *E. coli.* and affinity-purified using standard protocols. Briefly, 200 ml IPTG-induced cell culture pellet was lysed in 20 ml lysis buffer (containing 0.5% Triton-X-100) by sonication on ice. Centrifuge lysates were cleared by spinning at 10,000 x *g* for 30 minutes at 4 ºC. The supernatant was then incubated with 100 µl amylose resins or glutathione-sepharose beads at 4 ºC for 4 hrs with gentle rotation. The beads were then centrifuged and washed with lysis buffer for 3 times. Proteins were eluted with GST (10 mM reduced glutathione in 50 mM Tris. pH 8.0), or MBP (20 mM Tris-HCI, 200 mM NaCl, 1 mM EDTA, 1 mM DTT, 10 mM maltose, pH 7.4) buffer. The protein concentration was estimated by NanoDrop ND-1000 spectrophotometer and confirmed by the Bio-Rad Quick Start Bradford Dye Reagent. 10 µg of GST or GST fusion proteins (immobilized on glutathione-sepharose beads) were incubated with 10 µg prewashed MBP or MBP fusion proteins at 4 ºC in 150 µl of incubation buffer (10 mM HEPES at pH 7.5, 100 mM NaCl, 1 mM EDTA, 10% glycerol, and 0.5% Triton-X-100) for 1 hour. The beads were collected and washed three times with washing buffer (20 mM HEPES at pH 7.5, 300 mM NaCl, 1 mM EDTA, and 0.5% NP-40) and once with 50mM Tris.HCl (pH 7.5). Proteins in the beads were analyzed by immunoblot with an α-GST or α-MBP antibodies, respectively.

Vanadate-sensitive ATPase activity measurement

ATP hydrolysis by PM H^+-ATPase was measured in a vanadate-sensitive manner as previous described [22]. Briefly, the aerial parts of 14-day-old seedlings (Col-0, *tmk1-1,*

tmk4-1, and *tmk1-1 tmk4-1*) were incubated in KPSC buffer (10 mM potassium phosphate, pH 6.0, 2% sucrose, 50 μm chloramphenicol) in darkness for 10 hours. The buffer was replaced for every hour. The pretreated tissues were incubated in the presence of 10 μM IAA for 30 minutes in darkness. The tissues were homogenized with homogenization buffer (50 mM MOPS-KOH, pH 7.0, 100 mM KNO_3, 2 mM sodium molybdate, 0.1 mM NaF, 2 mM EGTA, 1 mM PMSF and 20 μM leupeptin) and the homogenates were centrifuged at 10,000 *g* for 10 minutes; the obtained supernatant was further ultra-centrifuged at 45,000 *g* for 60 minutes. The resultant pellet (microsomal fraction) was resuspended in the homogenization buffer. ATP hydrolytic activity of the microsomal fraction was measured in a vanadate-sensitive manner, and the inorganic phosphate released from ATP was measured [22].

***In vitro* phosphorylation**

Protoplasts were isolated from plants expressing AHA1-GFP as described above. Agarose immobilized (GFP-Trap beads, Chromotek, #gta-100) AHA1-GFP proteins was incubated with 1 μg MBP-TMK1KD or MBP-TMK1KDKm recombinant proteins (expressed in *E. coli* and isolated by affinity purification) in 100 μl phosphorylation buffer (5 mM HEPES, 10 mM $MgCl_2$, 10 mM $MnCl_2$, 1 mM DTT and 50 μM ATP)[16] at room temperature (24ºC) for 1 hr. After incubation, the reaction was stopped by adding 4 x SDS loading buffer. Proteins in the beads were analyzed by immunoblot with an α-pT947, α-AHA1-cat, or α-GFP antibodies (Chromotek, #3h9), respectively.

For the phosphorylation assays of the synthetic AHA1-C16 peptides, 10 μg synthetic peptides were incubated with 1 μg MBP-TMK1KD or MBP-TMK1KDKm recombinant proteins in 100 μl phosphorylation buffer for 1 hr before the samples were analyzed by mass spectrometry to determine the sites and the levels of AHA1-C16 phosphorylation.

476 **Primers for construct cloning and genotyping**

Purpose	Primers	sequences 5'-3'
Genotyping	*tmk1-1*LP*;*	CTCTGTTTCCACAACAGAGGC
	*tmk1-1*RP*;*	CCAGTGCCTGTGTTTAAGAGC
	*tmk4-1*LP;	TGCGATTGCTCAAAGAGGTCAGA
	*tmk4-1*RP;	GGCTGCATTGGTTGCACTGGAT
	ost2-2D-F	CTGGGCTGCTCACAAGAC
	ost2-2D-R	CTACACAGTGTAGTGATGTC
Protein		gtGGGGACAAGTTTGTACAAAAAAGCAGGCTTCATGCTCAACT
purification	AHA2-C-F	TGTTTGAG
		gtGGGGACCACTTTGTACAAGAAAGCTGGGTCCTACACAGTGT
	AHA2-C-R	AGTGAC
	TMK1-C-F	CGGATCCTTCTCAGGAAGTGAGAGCTC
	TMK1-C-R	CGAATTCTCATCGTCCATCTACTGAAGT
Transient		
Expression	AHA1-F-BamHI	CGGGATCCATGTCAGGTCTCGAAGATATC
in Protoplast	AHA1-R-SmaI	TCCCCCGGGCACAGTGTAGTGATGTCCTG
	AHA2-F-BamHI	CGGGATCCATGTCGAGTCTCGAAG
	AHA2-R-StuI	GAAGGCCTCACAGTGTAGTGACTGG
	TMK1-F-SpeI	GGACTAGTATGAAGAAAAGAAGAACC
	TMK1-R-StuI	GAAGGCCTTCGTCCATCTACTGAAGTG
	TMK1Km-F	TTCTCAGGAAGTGAGGCC TCAAATGCAGTAGTGGTG
	TMK1Km-R	CACCACTACTGCATTTGAGGCCTCACTTCCTGAGAA
Transient		gtGGGGACAAGTTTGTACAAAAAAGCAGGCTTC
Expression	AHA1-F	ATGTCAGGTC TCGAAGA
in tobacco		gtGGGGACCACTTTGTACAAGAAAGCTGGGTC
	AHA1-R	CACAGTGTAGTGATGTC
		gtGGGGACAAGTTTGTACAAAAAAGCAGGCTTC
	TMK1.Km-F	ATGAAGAAAAGAAGAACC

	gtGGGGACCACTTTGTACAAGAAAGCTGGGTC
TMK1.Km-R	TCGTCCATCTACTGAAGT
	gtGGGGACCACTTTGTACAAGAAAGCTGGGTCGAATCTCTTCTG
TMK1ext-R	CCTCTTTT

Acknowledgements

We thank members of the Yang laboratory for stimulating discussion and critical comments on this work. We are grateful to Dr. Jeffrey Leung (Department of Institute Jean-Pierre Bourgin, INRA, Versailles, France) for *ost2-2D* seeds, Dr. Koh Iba (Kyushu University, Japan) for *35S::GFP-AHA1* seeds, and Dr. Libo Shan (University of Texas A&M) for protoplast transient expression vectors. K.T. (20K06685) and T.K. (20H05687 and 20H05910) were funded by MEXT/JSPS KAKENHI. W.M.G was funded by NIH (GM067203). H.Z. was funded by NIH (S10OD016400).

References

1 McQueen-Mason, S., Durachko, D. M. & Cosgrove, D. J. Two endogenous proteins that induce cell wall extension in plants. *Plant Cell* 4, 1425-1433, doi:10.1105/tpc.4.11.1425 (1992).

2 Barbez, E., Dunser, K., Gaidora, A., Lendl, T. & Busch, W. Auxin steers root cell expansion via apoplastic pH regulation in Arabidopsis thaliana. *Proc Natl Acad Sci U S A* 114, E4884-E4893, doi:10.1073/pnas.1613499114 (2017).

3 Rayle, D. L. & Cleland, R. Enhancement of wall loosening and elongation by Acid solutions. *Plant physiology* 46, 250-253, doi:10.1104/pp.46.2.250 (1970).

4 Moloney, M. M., Elliott, M. C. & Cleland, R. E. Acid growth effects in maize roots: Evidence for a link between auxin-economy and proton extrusion in the control of root growth. *Planta* 152, 285-291, doi:10.1007/BF00388251 (1981).

5 Hager, A. Role of the plasma membrane H+-ATPase in auxin-induced elongation growth: historical and new aspects. *J Plant Res* 116, 483-505, doi:10.1007/s10265-003-0110-x (2003).

6 Haruta, M. *et al.* Molecular characterization of mutant Arabidopsis plants with reduced plasma membrane proton pump activity. *J Biol Chem* 285, 17918-17929, doi:10.1074/jbc.M110.101733 (2010).
7 Palmgren, M. G., Sommarin, M., Serrano, R. & Larsson, C. Identification of an autoinhibitory domain in the C-terminal region of the plant plasma membrane H(+)-ATPase. *J Biol Chem* 266, 20470-20475 (1991).
8 Ekberg, K., Palmgren, M. G., Veierskov, B. & Buch-Pedersen, M. J. A novel mechanism of P-type ATPase autoinhibition involving both termini of the protein. *J Biol Chem* 285, 7344-7350, doi:10.1074/jbc.M109.096123 (2010).
9 Jahn, T. *et al.* The 14-3-3 protein interacts directly with the C-terminal region of the plant plasma membrane H(+)-ATPase. *Plant Cell* 9, 1805-1814, doi:10.1105/tpc.9.10.1805 (1997).
10 Olsson, A., Svennelid, F., Ek, B., Sommarin, M. & Larsson, C. A phosphothreonine residue at the C-terminal end of the plasma membrane H+-ATPase is protected by fusicoccin-induced 14-3-3 binding. *Plant Physiol* 118, 551-555, doi:10.1104/pp.118.2.551 (1998).
11 Fuglsang, A. T. *et al.* Binding of 14-3-3 protein to the plasma membrane H(+)-ATPase AHA2 involves the three C-terminal residues Tyr(946)-Thr-Val and requires phosphorylation of Thr(947). *J Biol Chem* 274, 36774-36780, doi:10.1074/jbc.274.51.36774 (1999).
12 Svennelid, F. *et al.* Phosphorylation of Thr-948 at the C terminus of the plasma membrane H(+)-ATPase creates a binding site for the regulatory 14-3-3 protein. *Plant Cell* 11, 2379-2391, doi:10.1105/tpc.11.12.2379 (1999).
13 Maudoux, O. *et al.* A plant plasma membrane H+-ATPase expressed in yeast is activated by phosphorylation at its penultimate residue and binding of 14-3-3 regulatory proteins in the absence of fusicoccin. *J Biol Chem* 275, 17762-17770, doi:10.1074/jbc.M909690199 (2000).
14 Fendrych, M., Leung, J. & Friml, J. TIR1/AFB-Aux/IAA auxin perception mediates rapid cell wall acidification and growth of Arabidopsis hypocotyls. *Elife* 5, doi:10.7554/eLife.19048 (2016).
15 Spartz, A. K. *et al.* SAUR Inhibition of PP2C-D Phosphatases Activates Plasma Membrane H+-ATPases to Promote Cell Expansion in Arabidopsis. *Plant Cell* 26, 2129-2142, doi:10.1105/tpc.114.126037 (2014).
16 Cao, M. *et al.* TMK1-mediated auxin signalling regulates differential growth of the apical hook. *Nature* 568, 240-243, doi:10.1038/s41586-019-1069-7 (2019).
17 Huang, R. *et al.* Noncanonical auxin signaling regulates cell division pattern during lateral root development. *Proc Natl Acad Sci U S A* 116, 21285-21290, doi:10.1073/pnas.1910916116 (2019).
18 Xu, T. *et al.* Cell surface ABP1-TMK auxin-sensing complex activates ROP GTPase signaling. *Science* 343, 1025-1028, doi:10.1126/science.1245125 (2014).

19 Baral, A. *et al.* External Mechanical Cues Reveal a Katanin-Independent Mechanism behind Auxin-Mediated Tissue Bending in Plants. *Developmental cell* 56, 67-80 e63, doi:10.1016/j.devcel.2020.12.008 (2021).
20 Wang, Q. *et al.* A phosphorylation-based switch controls TAA1-mediated auxin biosynthesis in plants. *Nat Commun* 11, 679, doi:10.1038/s41467-020-14395-w (2020).
21 Xu, T. *et al.* Cell surface- and rho GTPase-based auxin signaling controls cellular interdigitation in Arabidopsis. *Cell* 143, 99-110, doi:10.1016/j.cell.2010.09.003 (2010).
22 Takahashi, K., Hayashi, K. & Kinoshita, T. Auxin activates the plasma membrane H+-ATPase by phosphorylation during hypocotyl elongation in Arabidopsis. *Plant Physiol* 159, 632-641, doi:10.1104/pp.112.196428 (2012).
23 Dai, N., Wang, W., Patterson, S. E. & Bleecker, A. B. The TMK subfamily of receptor-like kinases in Arabidopsis display an essential role in growth and a reduced sensitivity to auxin. *PLoS One* 8, e60990, doi:10.1371/journal.pone.0060990 (2013).
24 Falhof, J., Pedersen, J. T., Fuglsang, A. T. & Palmgren, M. Plasma Membrane H(+)-ATPase Regulation in the Center of Plant Physiology. *Mol Plant* 9, 323-337, doi:10.1016/j.molp.2015.11.002 (2016).
25 Kinoshita, T. & Shimazaki, K. Blue light activates the plasma membrane H(+)-ATPase by phosphorylation of the C-terminus in stomatal guard cells. *EMBO J* 18, 5548-5558, doi:10.1093/emboj/18.20.5548 (1999).
26 Kerkeb, L., Venema, K., Donaire, J. P. & Rodriguez-Rosales, M. P. Enhanced H+/ATP coupling ratio of H+-ATPase and increased 14-3-3 protein content in plasma membrane of tomato cells upon osmotic shock. *Physiol Plant* 116, 37-41, doi:10.1034/j.1399-3054.2002.1160105.x (2002).
27 Niittyla, T., Fuglsang, A. T., Palmgren, M. G., Frommer, W. B. & Schulze, W. X. Temporal analysis of sucrose-induced phosphorylation changes in plasma membrane proteins of Arabidopsis. *Mol Cell Proteomics* 6, 1711-1726, doi:10.1074/mcp.M700164-MCP200 (2007).
28 Han, J. & Burgess, K. Fluorescent indicators for intracellular pH. *Chem Rev* 110, 2709-2728, doi:10.1021/cr900249z (2010).
29 Merlot, S. *et al.* Constitutive activation of a plasma membrane H(+)-ATPase prevents abscisic acid-mediated stomatal closure. *EMBO J* 26, 3216-3226, doi:10.1038/sj.emboj.7601750 (2007).
30 Fu, Y., Xu, T., Zhu, L., Wen, M. & Yang, Z. A ROP GTPase signaling pathway controls cortical microtubule ordering and cell expansion in Arabidopsis. *Curr Biol* 19, 1827-1832, doi:10.1016/j.cub.2009.08.052 (2009).
31 Ren, H., Park, M. Y., Spartz, A. K., Wong, J. H. & Gray, W. M. A subset of plasma membrane-localized PP2C.D phosphatases negatively regulate SAUR-mediated cell expansion in Arabidopsis. *PLoS Genet* 14, e1007455, doi:10.1371/journal.pgen.1007455 (2018).

32 Spartz, A. K. *et al.* The SAUR19 subfamily of SMALL AUXIN UP RNA genes promote cell expansion. *Plant J* 70, 978-990, doi:10.1111/j.1365-313X.2012.04946.x (2012).
33 Fendrych, M. *et al.* Rapid and reversible root growth inhibition by TIR1 auxin signalling. *Nat Plants* 4, 453-459, doi:10.1038/s41477-018-0190-1 (2018).
34 Prigge, M. J. *et al.* Genetic analysis of the Arabidopsis TIR1/AFB auxin receptors reveals both overlapping and specialized functions. *eLife* 9, doi:10.7554/eLife.54740 (2020).
35 Chen, J. & Yang, Z. Novel ABP1-TMK auxin sensing system controls ROP GTPase-mediated interdigitated cell expansion in Arabidopsis. *Small GTPases* 5 (2014).
36 Marques-Bueno, M. M. *et al.* Auxin-Regulated Reversible Inhibition of TMK1 Signaling by MAKR2 Modulates the Dynamics of Root Gravitropism. *Curr Biol* 31, 228-237 e210, doi:10.1016/j.cub.2020.10.011 (2021).
37 Clough, S. J. & Bent, A. F. Floral dip: a simplified method for Agrobacterium-mediated transformation of Arabidopsis thaliana. *Plant J* 16, 735-743, doi:10.1046/j.1365-313x.1998.00343.x (1998).
38 Hayashi, Y. *et al.* Biochemical characterization of in vitro phosphorylation and dephosphorylation of the plasma membrane H+-ATPase. *Plant Cell Physiol* 51, 1186-1196, doi:10.1093/pcp/pcq078 (2010).
39 Hayashi, M., Inoue, S., Takahashi, K. & Kinoshita, T. Immunohistochemical detection of blue light-induced phosphorylation of the plasma membrane H+-ATPase in stomatal guard cells. *Plant Cell Physiol* 52, 1238-1248, doi:10.1093/pcp/pcr072 (2011).
40 Thakur, J. K., Tyagi, A. K. & Khurana, J. P. OsIAA1, an Aux/IAA cDNA from rice, and changes in its expression as influenced by auxin and light. *DNA Res* 8, 193-203, doi:10.1093/dnares/8.5.193 (2001).
41 Yoo, S. D., Cho, Y. H. & Sheen, J. Arabidopsis mesophyll protoplasts: a versatile cell system for transient gene expression analysis. *Nature protocols* 2, 1565-1572, doi:10.1038/nprot.2007.199 (2007).

Extended Data

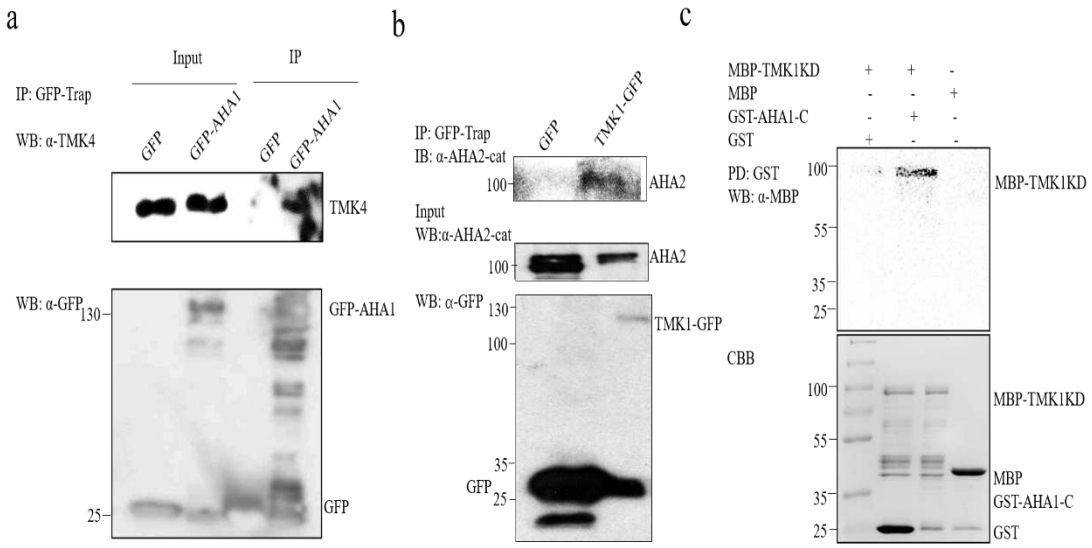

Extended Data Fig. 1. TMK interacts with AHAs *in planta* and *in vitro*. **a,** TMK4 associates with AHA1 in transgenic plants. The membrane proteins from 4-week-old *35S::GFP* only and *35S::GFP-AHA1* plants were immunoprecipitated with α-GFP-Trap antibody and analyzed with Western blots using an α-TMK4 antibody (Top). The expression of GFP-AHA1 and GFP control in transgenic plants is shown (Bottom). **b,** TMK1 associates with AHA2 in transgenic plants. Membrane proteins from 4-wk-old *35S::GFP* and *pTMK1::TMK1-GFP/tmk1-1/4-1* transgenic plants were immunoprecipitated with α-GFP-Trap antibody and analyzed with Western blots using an α-AHA2 antibody (Top). The expression of TMK1-GFP and GFP control in transgenic plants is shown (Bottom). **c**, TMK1's cytoplasmic kinase domain (KD) interacts with AHA2's C-terminal domain *in vitro*. *E. coli*-expressed maltose-binding protein (MBP)-TMK1KD or MBP proteins were incubated with glutathione bead-bound glutathione-S-transferase (GST)-AHA2-C or GST (Pull-down:GST), and the beads were collected and washed for Western blotting of immunoprecipitated proteins with α-MBP antibody (left). The input GST-AHA2-C, MBP-TMK1KD, MBP, and GST proteins were detected by Coomassie brilliant blue staining (CBB).

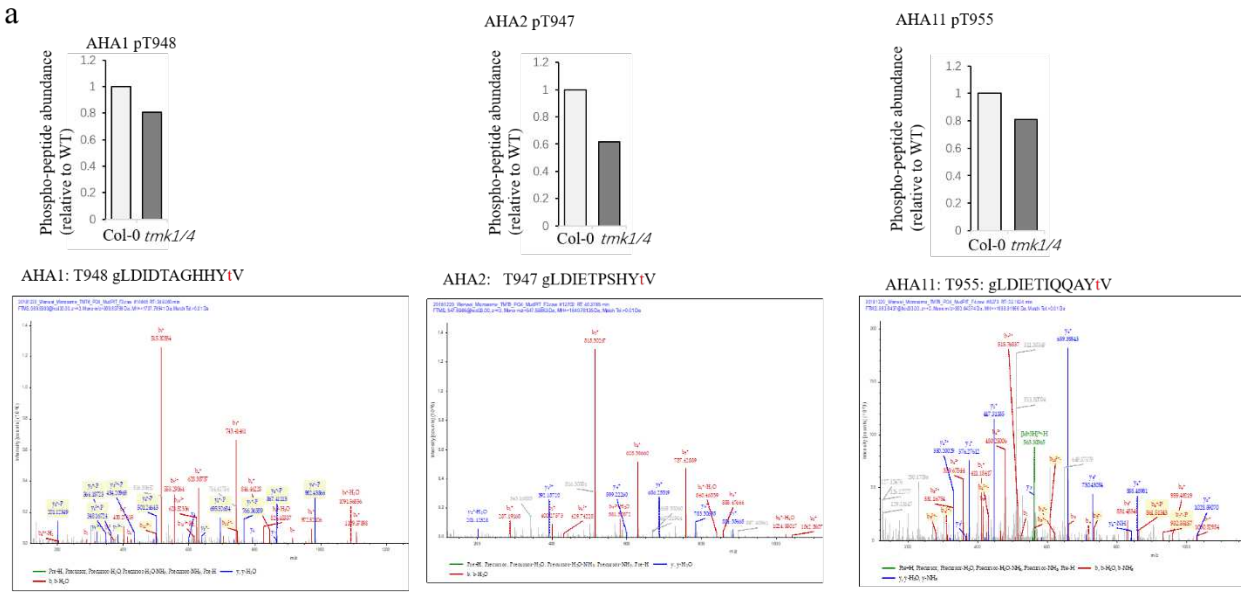

638

Annotated Sequence	Modifications	Master Protein Accessions	Delta Score	m/z [Da]	MH+ [Da]	DeltaM [ppm]	Deltam/z [Da]	XCorr	Percolator q-Value	Percolator PEP	Quan Result ID	Reporter Quan Info	TMT126	TMT128
[K].gLDIDTAGHHYtV.[-]	N-Term(TMT6plex); T12(Phospho)	AT2G18960.1 AHA1	0.0231	854.4015	1707.796	0.95	0.00081	3.47	0.000664	0.003404	164530	Unique	152.4	121.1
[K].gLDIETPSHYtV.[-]	N-Term(TMT6plex); T11(Phospho)	AT4G30190.2 AHA2	0.0149	820.8954	1640.783	3.94	0.00323	2.68	0.00102	0.01205	186811	Unique	109	83.4
[K].gLDIETIQQAYtV.[-]	N-Term(TMT6plex); T12(Phospho)	AT5G62670.1 AHA11	0.1501	880.4432	1759.879	4.21	0.00371	4.73	0	0.000163	169325	Unique	109.5	68.9

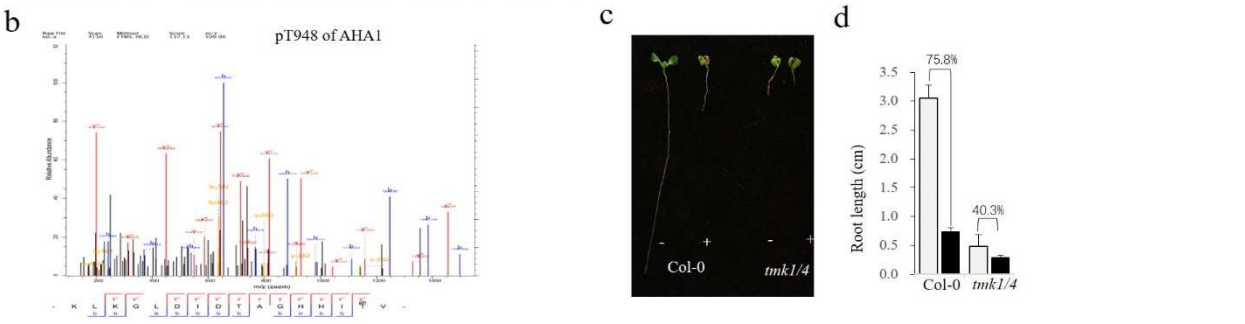

639

640 **Extended Data Fig. 2. TMK1 and TMK4 impact the phosphorylation status of AHAs and**
641 **the function of the PM H^+-ATPase pump.** **a,** The phosphorylated status of AHAs were
642 changed in the *tmk1-1 tmk4-1* (*tmk1/4)* mutant. The aerial part of 5-days auxin-depleted seedlings
643 was used to prepare membrane proteins for TMT (Tandem mass tag) labelling and mass
644 spectrometry quantification as described in Method. Mass spectrometry analysis showed that the
645 abundance of the peptides containing phosphorylated penultimate threonine from AHA1, AHA2,
646 and AHA11 was significantly decreased in *tmk1-1 tmk4-1* (*tmk1/4*) mutant relative to wild type.
647 High-resolution fragmentation spectra of peptides containing phosphorylated penultimate
648 threonine are presented in the middle, phosphorylated peptides mass spectrometry information is
649 presented at the bottom. **b**, High-resolution fragmentation spectra of peptides containing
650 phosphorylated penultimate threonine of AHA1-C16 synthetical peptide (pT948 of AHA1) (see
651 Fig. 2d). **c,** Lithium tolerance in the *tmk1-1 tmk4-1* (*tmk1/4*) mutant. Wild type (Col-0) and
652 *tmk1-1 tmk4-1* (*tmk1/4*) mutant seedlings were grown on 1/2 MS medium with or without 18 mM
653 LiCl for 5 days. LiCl treatment caused severe seedling growth retardation and severe chlorosis of

the aerial parts in Col-0, whereas the *tmk1-1 tmk4-1* (*tmk1/4*) mutant was tolerant to LiCl, especially in the aerial parts. **d**, The root length of the seedlings was measured by ImageJ. Error bar represents SEM (n>10 hypocotyls per line). The number above the columns indicates the percentage of root growth inhibition induced by LiCl.

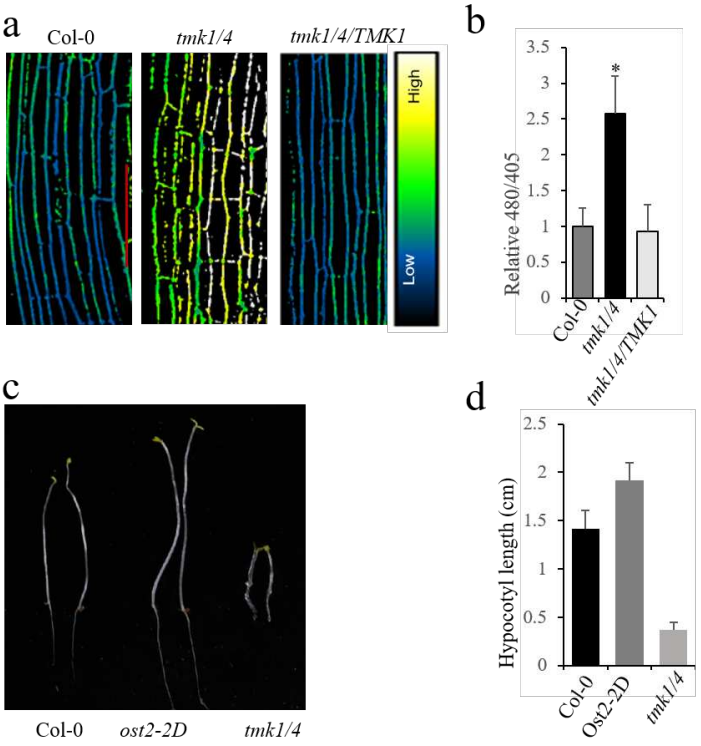

Extended Data Fig. 3. TMK1 and TMK4 regulate apoplastic pH and hypocotyl elongation. **a**, TMK1 (*pTMK1::TMK1-GFP*) complemented the apoplastic pH defect of the *tmk1-1 tmk4-1* (*tmk1/4*) mutant. Comparison of the apoplastic pH in WT, the *tmk1-1 tmk4-1* mutant, and the *tmk1-1 tmk4-1/TMK1* (*tmk1/4/TMK1*) complemented line. Visualized by HPTS staining (a). Y-Axis: the mean 458/405 values of the *tmk1-1 tmk4-1* mutant and the *TMK1* complemented line relative to wild type (b). **c** and **d**, The *tmk1-1 tmk4-1* mutant showed a defect in hypocotyl elongation (c). Hypocotyl lengths of 3 days-old etiolated seedlings were measured by Image J (d). Error bar represents SD (n>10 hypocotyls per line). Scale bar= 100 μM.

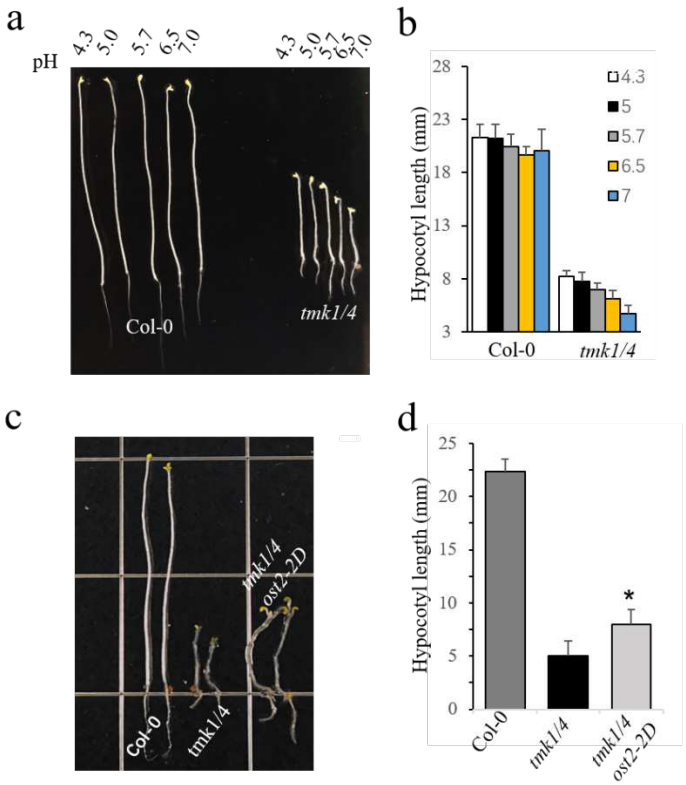

668

669 **Extended Data. Fig. 4. Acidic environments and activation of the PM H^+-ATPase pump**
670 **partially restored hypocotyl elongation defect in *tmk1-1 tmk4-1*.** **a** and **b**, Low pH in the
671 medium was able to partially restore the *tmk1-1 tmk4-1* (*tmk1/4*) defect in hypocotyl elongation.
672 Seedlings growth on 1/2 MS medium with indicated pH (a), and the length was measured by
673 ImageJ (b). **c** and **d**, *ost2-2D* mutation partially restored the hypocotyl elongation defect of *tmk1-1*
674 *tmk4-1* mutant. Seedlings were grown on 1/2 MS medium for 4 days, and the length was measured
675 by ImageJ. Values are means ±SD; Error bar represents SD (n>20 hypocotyl per line), * P ⩽
676 0.05.

677

Figures

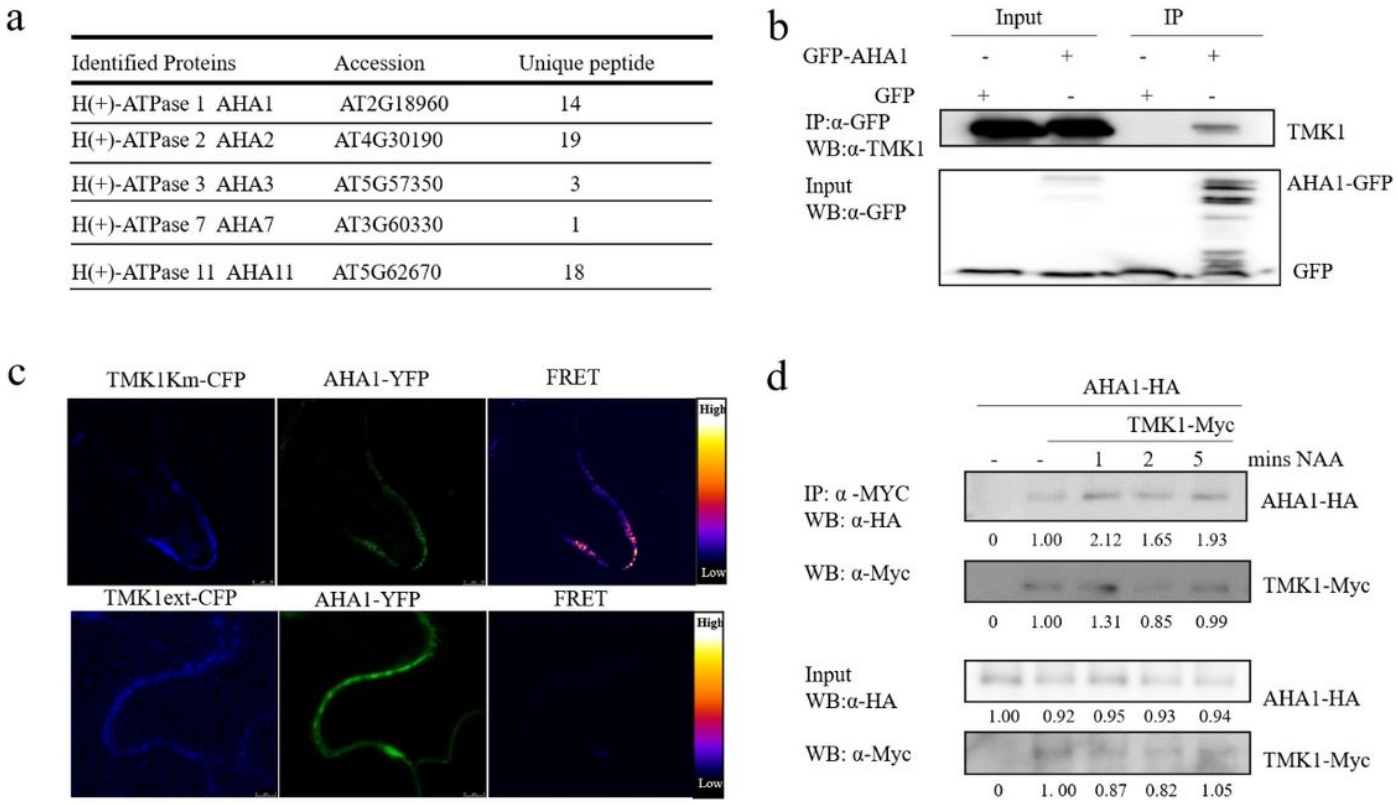

Figure 1

TMK1 directly interacts with AHAs. a, Summary of LC-MS/MS analysis of AHAs associated with TMK1-GFP. The number of unique AHA peptides identified in the 99 immunoprecipitates from pTMK1::TMK1-GFP transgenic seedlings is shown. IP-MS did not identify any AHA peptides from control pTMK1::GFP seedlings. b, co-immunoprecipitation of TMK1 with AHA1 in transgenic plants. Membrane proteins from 4-week-old 35S::GFP and 35S::GFP-AHA1 plants were immunoprecipitated with α-GFP-Trap antibody and analyzed with Western blotting using an α-TMK1 antibody (Top). The expression of AHA1-GFP and GFP control in transgenic plants is shown in the bottom panel. The experiments were repeated three times with similar results. c, TMK1 interacted with AHA1 on the PM. FRET analysis in Nicotiana benthamiana leaf epidermal cells transiently co-expressing TMK1Km-CFP and AHA1-YFP showed TMK1Km-CFP directly interacted with AHA1-YFP on the PM. The transient expression was achieved by agrobacterium infiltration. The extracellular domain of TMK1 (TMK1ext-CFP) did not interact with AHA1-YFP in N. benthamiana. More than 10 cells were determined with similar results. d, TMK1's association with AHA1 in Arabidopsis protoplasts was rapidly enhanced by auxin treatments within 1 minute. TMK1-Myc was co-expressed with AHA1-HA in Arabidopsis protoplasts. Co-IP was carried out with an α-Myc antibody (IP: α-Myc), and the proteins were analyzed by using Western blot with an α-HA antibody. Top shows that AHA1-HA coimmunoprecipitated with TMK1-Myc (IP: α-Myc; WB: α-HA, WB: α-Myc). The Middle and Bottom show the expression of AHA1-HA and TMK1-Myc proteins, respectively

(WB: α-HA or α-Myc for input control). Protoplasts were treated with 1 μM NAA for 1, 2, and 5 minutes as indicated. The number under the immunoblot is the relative signal intensities as determined by ImageJ. Similar results were reproduced twice in experiments involving 2 min and 5 min NAA treatments.

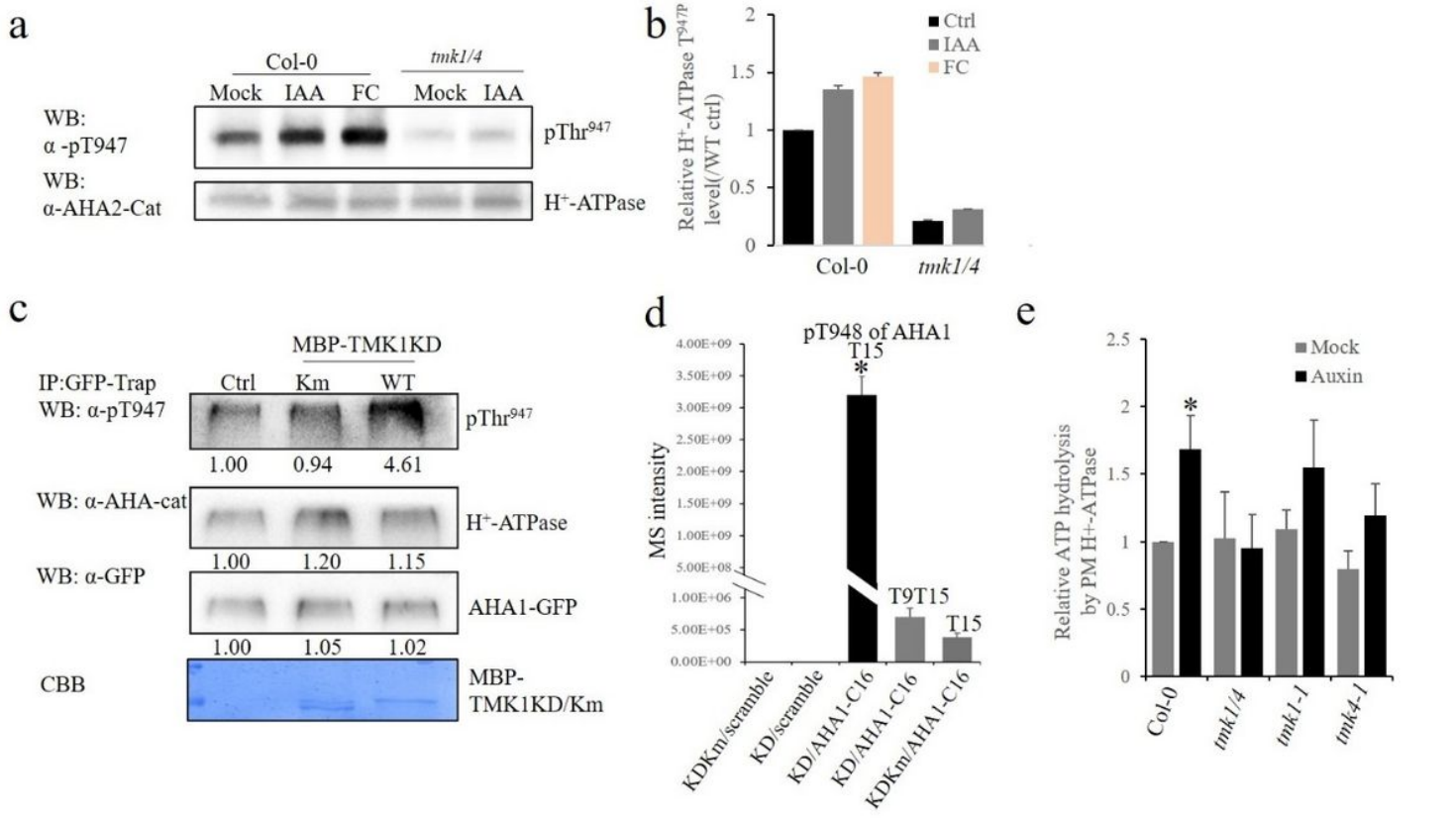

Figure 2

TMK1 and TMK4 are required for auxin-induced phosphorylation and activation of the PM H +-ATPase. a, Auxin-induced AHA phosphorylation is compromised in the tmk1-1 tmk4-1(tmk1/4) mutant. The endogenous auxin-depleted aerial sections of seedlings were incubated with 100 nM IAA for 10 minutes or 10 μm fusicoccin (FC) for 5 minutes, respectively. The amounts of H + -ATPase and the phosphorylation status of the penultimate Thr in the C terminus were determined by immunoblot analysis with anti-H +-ATPase (H +-ATPase) and anti pThr-947 (pThr 947) antibodies, respectively. b, Quantification of the phosphorylation level of the H + -ATPase. Values are means ± SD; n = 3 independent experiments. c, MBP-TMK1KD phosphorylated AHA1-GFP in vitro. AHA1-GFP was transiently expressed in Arabidopsis protoplasts and immunoprecipitated by GFP-trap. The GFP-trap beads immobilized AHA1 proteins were incubated with TMK1 (TMK1KD, WT) or kinase-dead form (TMK1KD,Km) for 1 hr. The amounts of H+-ATPase and phosphorylated penultimate Thr were determined by immunoblot analysis with anti-H+-ATPase (H+-ATPase) and anti-pThr-947 (pThr 947) antibodies, respectively. The AHA1-GFP proteins were determined by immunoblot analysis with an anti-GFP antibody. The input MBP-TMK1KD and MBP-TMK1KDKm recombinant proteins were detected by coomassie brilliant blue staining (CBB). The number under the immunoblot is the relative signal intensities as determined by ImageJ. d, MBP-

TMK1KD phosphorylated the synthetic AHA1-C16 peptide in vitro. MBP-TMK1KD or MBP-TMK1KDKm (1 µg) was incubated with the AHA1-C terminal synthetic peptide (KLKGLDIDTAGHHITV) or a scrambled peptide (GDAHVKITHLDKGLIT) (10 µg) in 100 µl phosphorylation buffer, respectively. The peptides were then analyzed by mass spectrometry. The graph shows the abundance of phosphorylated peptides at the indicated residues analyzed mass spectrometry. Values are means ±SD; n =3. * $P \leq 0.01$, results of One-way ANOVA-tests. Two biological replicates with three technical replicates/each produced similar results. e, Auxin induction of H+-ATPase activity in the aerial parts of wild type and the tmk1-1 tmk4-1 mutant. Aerial sections 208 of 14-days old seedlings were treated with 10 µm IAA for 30 minutes and used for vanadate-sensitive ATP hydrolysis assay by determining the inorganic phosphate released from ATP as described previously 25. The values shown are relative ATP hydrolytic activity of indicated samples to that of control Col-0 without auxin treatment. Values are means ± SD; n =3. * $P \leq 0.05$, results of paired Student's t-tests.

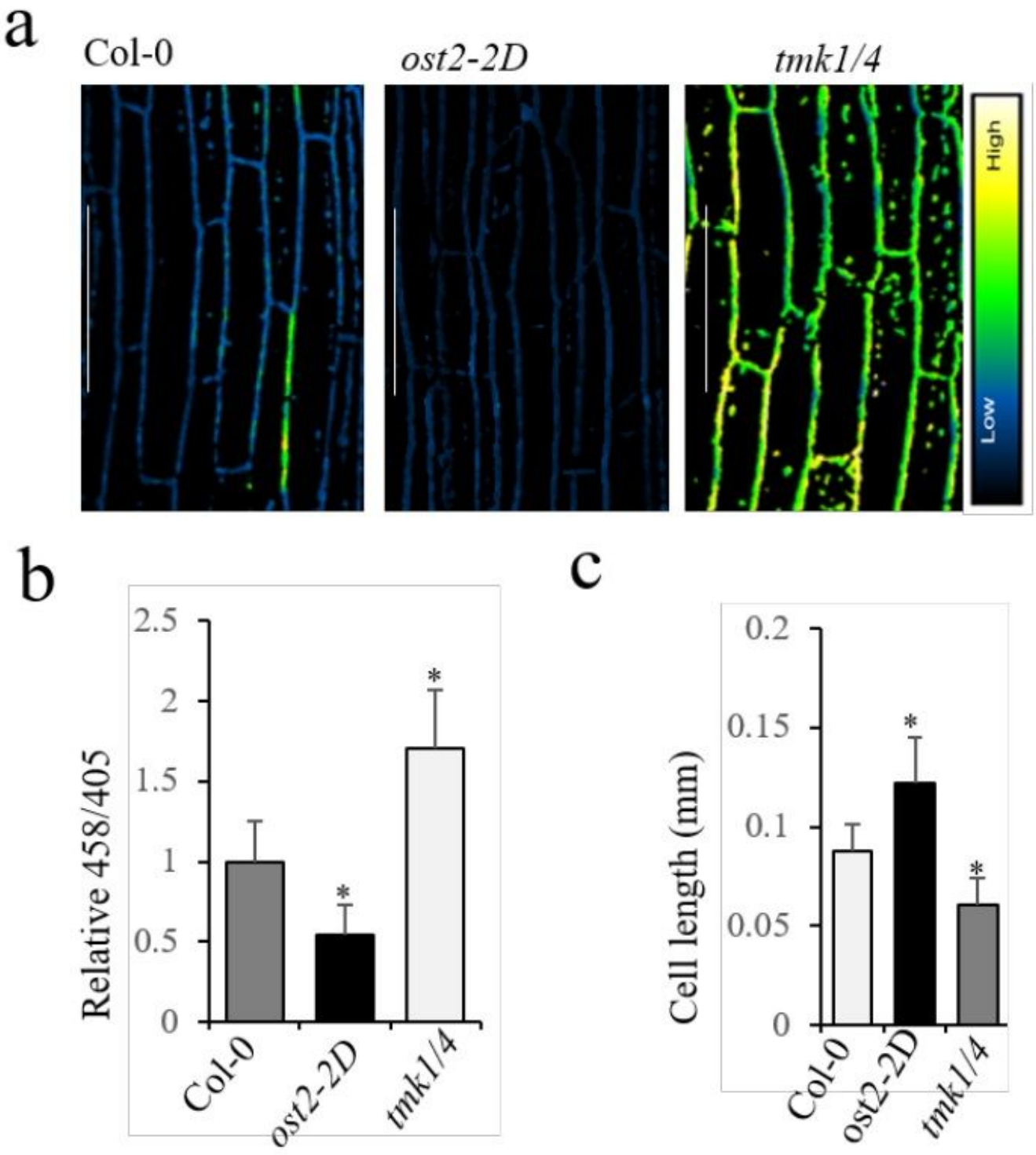

Figure 3

TMK1 and TMK4 are required for apoplastic acidification and cell elongation in Arabidopsis hypocotyl. a and b, Comparison of the apoplastic pH in wild type (Col-0), ost2-2D, and the tmk1-1 tmk4-1 (tmk1/4) mutant. Changes in pH were visualized with ratiometric values of fluorescent HPTS. Y-Axis: the mean 458/405 values of ost2-2D and the tmk1-1 tmk4-1 mutant relative to the WT. c, Epidermal cell lengths of hypocotyls from two days-old etiolated seedlings were measured using Image J. Hypocotyl epidermal

cells in the 100-500 μM region after apical hook were measured. Values are means ±SD; (n>20 cells per line). * P≤0.05. Scale bar=100 μM